CHEMICAL ENGINEERING TRANSACTIONS
VOL. 44, 2015
A publication of AIDIC
The Italian Association of Chemical Engineering
Online at www.aidic.it/cet
Guest Editors: Riccardo Guidetti, Luigi Bodria, Stanley Best

ISBN 978-88-95608-35-8; **ISSN** 2283-9216

Characterizing Physical States of Agricultural Products Using Magnetic Resonance Imaging

Seong Min Kim

Department of Bioindustrial Machinery Engineering, Chonbuk National University, 567 Baekje-daero, Deokjin-gu, Jeonju-si, Jeollabuk-do, Republic of Korea
smkim@jbnu.ac.kr

Magnetic resonance imaging (MRI) has been successfully utilized to examine or to measure various internal physical and chemical parameters including chemical components, internal disorders, and internal structure in agricultural products. MRI techniques can be applied to the most agricultural products in a noninvasive nondestructive way. Additionally, various factors related to the quality of agricultural products can be measured at the same time from the target sample. In this study, fresh fruits such as mature and immature figs, persimmon, grape, mango, and dragon fruit were investigated using an industrial grade 1 T MRI system to estimate their magnetic resonance parameters and to characterize their physical states. Multi-slice multi-echo pulse sequences were used to investigate region of interest (ROI) in samples. Magnetic resonance parameters from a series of magnetic resonance images with different echo times (TEs) at different locations of the sample were acquired. Magnetic resonance parameters estimated mono-exponential and bi-exponential curve fitting were closely related to the physical states of fruit samples. This method suggests a useful way to contrast region of interest (ROI) in a simple way when we are using MRI as an investigating tool.

1. Introduction

The demands on the quality of agricultural and food products are very high. Quality evaluation has been primarily performed by examining external factors such as color, scars, defects and insect damage. However, internal factors such as structure, maturity, texture, chemical components and internal defects or damages are key points in quality evaluation of agricultural and food products. Due to advance of technology, there are many nondestructive internal quality evaluation methods available now. Most of current nondestructive internal quality evaluation methods based on optical, spectroscopic, and mechanical techniques cannot measure internal quality factors effectively (Butz et al., 2005).
Nuclear magnetic resonance (NMR) techniques can be applied to various biosystems such as agricultural products, food and biomedical tissues due to its non-destructive and non-contacting nature (Gadian, 1995). Magnetic resonance imaging (MRI), which is the extension of the two-dimensional NMR, is now intensively used in medical area and applied to high moisture biosystems such as fruits, livestock products and food (Chen et al., 1989). This technique is presently utilized as a tool to refine theoretical models for improving food processes such as canning, freezing, frying, drying, form and emulsion formulation, crystallization, and extrusion processes in food or chemical engineering areas (McCarthy, 1994). Magnetic resonance (MR) methods are particularly well-suited for assessing the quality of fruit because of the abundance of protons in these biological materials. Various types of experimental approaches using MRI technique were used by many researchers. On-line quality evaluation magnetic resonance sensors were developed (Kim et al., 1999). Andaur et al. (2004) used MRI to investigate the growth and ripening state of wine grapes. Freeze damage of mandarin orange was examined and a method to sort freeze damaged oranges was suggested (Kim et al., 2008). Processed tomatoes were investigated combined with multivariate image analysis (Milczarek, 2009) using MRI technique. Zhang and McCarthy (2013) used magnetic resonance techniques to predict the pomegranate quality attributes and concluded that MRI can evaluate multiple quality parameters in a single

measurement. Defraeye et al. (2013) utilized MRI technique to characterize different types of apple tissues and found that magnetic resonance parameters varied with physical state of tissue.
The objectives of this study were to investigate fresh fruits using an industrial grade MRI system to measure their magnetic resonance parameters and to examine the relationship between magnetic resonance parameters and physical states of fresh fruits.

2. Materials and method

2.1 Samples

Various fresh fruits such as fig, 'Fuyu' persimmon, grape, mango, and dragon fruit were used in this study. Grape, mango, and dragon fruit were purchased at a local market in Davis, CA, USA. Mature fig, immature fig, and persimmon were handpicked at the University of California, Davis, CA, USA. All samples were selected to fit into an imaging coil except dragon fruit. Dragon fruit was cut suitable for experiment.

2.2 Magnetic resonance imaging

MRI data was acquired using a 1 T industrial grade MRI system (ASPECT Magnetic Technologies Ltd., Israel) which is self-shielded. This magnet has no fringe magnetic fields, enabling us to use in an industrial environment. A sample holder made of Plexiglas was mounted in the center of a 90 mm inner diameter imaging probe. The sample holder was used to place a sample in the middle of the NMR coil consistently. Table 1 gives MRI pulse sequence parameters used in the study. A multi-slice multi-echo (MSME) imaging pulse sequence with 8 ms echo time (TE) and 2000 ms repetition time (TR) was used to acquire images from 8 slices. MSME was used to map spin-spin relaxation time constant (T_2) of slices of a sample with 64 different TEs, which were set to 8, 16, …, 512 ms. Image slice thickness was 0.5 mm and field of view (FOV) was 64 mm. The image pixel size was set to 128 x 128, so the spatial in-plane resolution of a voxel (volume element) is 125 μm^3.

Table 1: MRI pulse sequence parameters

Pulse sequence	Multi-slice multi-echo
Field of view (mm^2)	64x64
Image size($pixel^2$)	128x128
Slice thickness (mm)	0.5
Repetition time (TR) (ms)	2,000
Echo time (TE) (ms)	8, 16, …, 512
No. of images	64

2.3 Data analysis

A custom MRI data analysis program was programmed using a commercial programming software (MATLAB 2013b for Windows, Mathworks, USA). The MRI data analysis program functions as follow. First, it displays MR images of all slices. Second, the user selects the slice of interest and it displays image of the selected slice. Third, the user selects region of interest (ROI) with mouse on the window screen. Finally, it processes data in the ROI and displays processed MR mapping images and histograms showing distribution of magnetic resonance parameters. So a total of 6 MR mapping images, i.e. T_2 and M_o by mono-exponential fitting and T_{21}, T_{22}, M_{o1} and M_{o2} by bi-exponential fitting, and their histograms are generated. Calculations of MR values were carried out by employing a mono- and bi-exponential least-squares fit. The calculated spin-spin relaxation time constant was fitted by mono-exponential or bi-exponential decay curve according to the Eq(1).

$$M(t) = \sum_i M_{0,i} \exp\left(-\frac{t}{T_{2,i}}\right) + M_\infty \quad (1)$$

where $M_{0,i}$ is the magnitude of the *i*th exponential, t is the echo time, $T_{2,i}$ is the characteristic spin-spin relaxation time constant (T_2) for the *i*th exponential and M_∞ is the residual noise.

3. Results and discussion

Total of 6 fresh fruits, mature fig, immature fig, persimmon, grape mango, and dragon fruit, were examined. MSME pulse sequence was successfully applied and acquired MR parameters in a two-dimensional plane. We can assume that there are two water states, free and bound water. Free water generates longer T_2 value compared with bound water. Magnitude, M_o, of signal relates to the amount of water in a ROI of magnetic resonance image. T_2 value is more related to chemical environment than M_o. So, we can characterize the physical state of sample using magnetic resonance parameters, T_2 and M_o, using MRI. Table 2 shows average values of estimated relaxation time constant, T_2, and magnitude, M_o, from ROI of samples. Each sample shows different MR values as expected because each sample has its own unique tissue structure and chemical components.

Relatively high moisture content fruits such as grape and dragon fruit whose moisture contents are more than 85% show high T_2 values. Majority of water is in the free state. However, low T_2 values were observed in figs. It is expected that most of water is in the bounded state in figs. Mature and immature figs show interesting results. T_2 values of the rind part are different but M_o is almost same with different maturity stages. Also, mean T_2 values from the whole part shows difference. Usually, inner parts generate longer T_2 values than outer parts close to rind, except in persimmon. Persimmon, which has a vascular system in the center of the fruit, generates shorter T_2 values from the inner than from outer part. The rind part of mature dragon fruit generates longer T_2 value than the flesh tissue but M_o values are not. This means that the amount of water is small but more free water is in rind part than flesh part.

Table 2: Average values of calculated relaxation time constant, T_2, in ms and magnitude of image intensity Each value represents mean ± standard deviation

Sample	Part	T_2	T_{21}	T_{22}	M_o	M_{o1}	M_{o2}
Mature fig	Whole	77±9.2	77±9.7	97±180	2,435±846	2,365±833	89±223
	Rind	74±6.6	74±6.6	64±30	1,349±421	1,325±414	37±83
	Flesh(outer)	69±4.9	69±4.9	70±66	2,554±190	2,495±196	76±135
	Flesh(inner)	88±4.6	88±5.8	173±304	3,272±222	3,181±308	106±244
Immature fig	Whole	63±13	86±30	61±143	2,233±616	1,498±319	960±485
	Rind	49±4.1	51±8.7	157±279	1,349±223	1,125±236	258±251
	Flesh(outer)	60±7.5	83±16	34±62	2,353±282	1,528±209	1,073±219
	Flesh(inner)	79±5.9	123±13	32±3.1	2,950±165	1,879±99	1,479±81
Persimmon	Whole	128±9.4	128±9.4	129±74	3,297±623	3,134±643	163±72
	Flesh(outer)	131±3.2	133±2.2	13±20	3,559±165	3,531±185	136±220
	Flesh(inner)	115±4.6	115±4.6	115±4.6	2,356±306	2,189±316	167±28
Grape	Whole	216±45	396±299	76±86	1,783±439	1,560±476	693±421
Mango	Whole	164±18	164±18	120±73	1,136±107	1,108±106	35.4±51
	Flesh	178±8.5	178±8.4	50±79	1,080±106	1,067±99	87±152
	Seed	144±8.4	144±8.4	128±49	1,105±114	1,081±111	25±21
Dragon fruit	Whole	243±47	264±102	33±81	2,882±1,044	2,892±1,024	195±300
	Rind	275±37	302±67	8.3±29	1,835±446	1,845±432	4,353±37
	Flesh	205±16	205±16	32±76	3,861±198	3,860±199	2±6.6

Figure 1, Figure 3, and Figure 5 show processed T_2 mapping images and histograms of mature fig, immature fig, and persimmon, respectively. Figure 2, Figure 4, and Figure 6 show processed M_o mapping images and histograms of the respective samples. Processed mapping of the two-dimensional image gives spatial distribution information of T_2 and M_o from a sample. Histogram delivers the distribution and frequency of calculated T_2 and M_o values. In contrast to T_2 mapping images, M_o mapping images clearly show the difference between the properties of the fig samples in the two developmental stages (Figure 1, Figure 2, Figure 3, and Figure 4). We can expect that the physical and chemical environment changes when fig fruit matures. Analysis of M_o histogram pattern provides a better indicator of variations of the physical state than T_2 analysis. We can observe that the two major peaks, which indicate two major components, of M_o histogram from the immature fig sample change to the three major peaks of M_o histogram from the mature fig sample (Figure 2 and Figure 4). Histogram analysis is easier to understand change of physical states than examining mapping images. However, analyzing persimmon shows opposite result. T_2 analysis is easier to understand physical state change than M_o analysis (Figure 5, and Figure 6). So we can conclude that we have to choose a right analysis method, T_2 or M_o analysis method, suitable to a target sample after examining the its histograms.

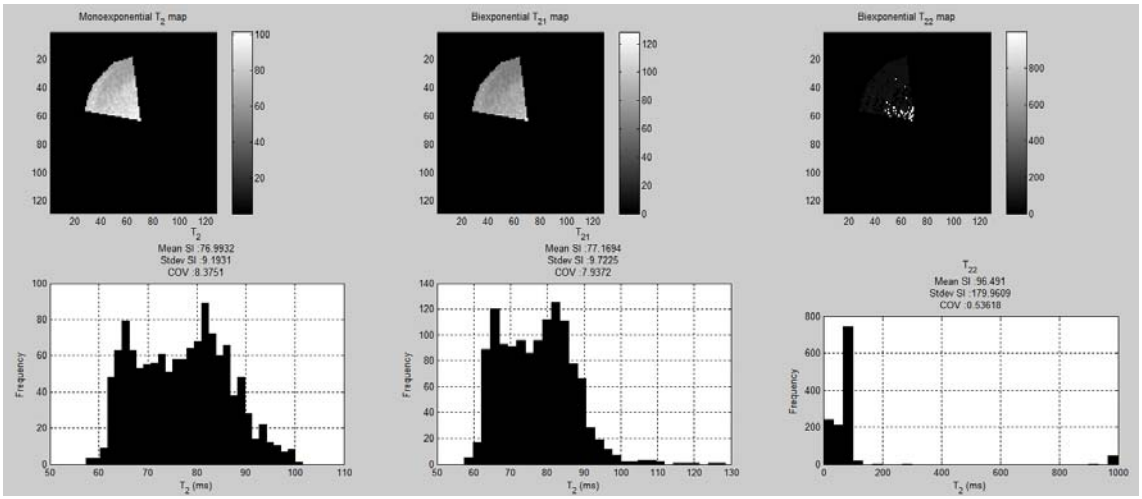

Figure 1: Processed T_2, T_{21}, and T_{22} mapping images (top) and histograms (bottom) of mature fig

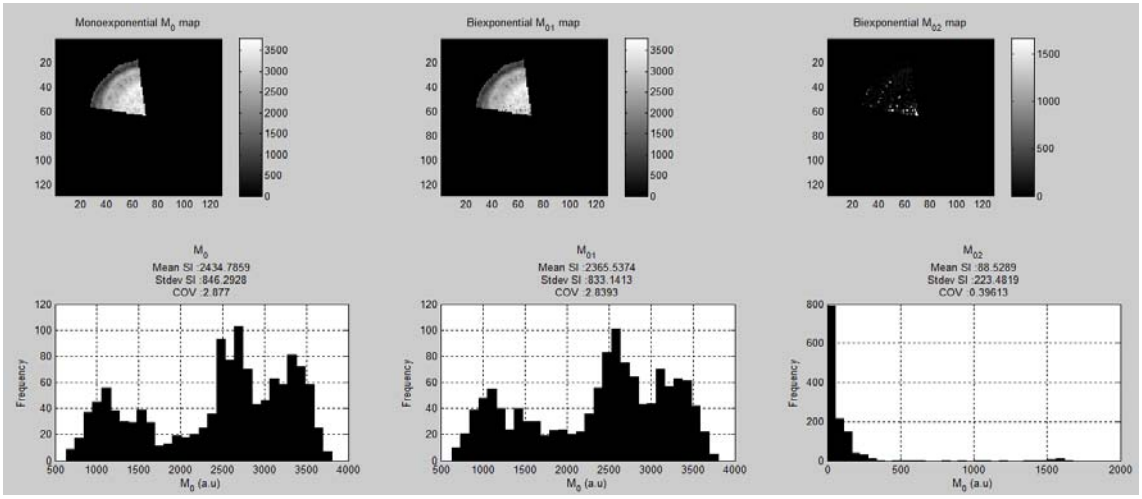

Figure 2: Processed M_0, M_{21}, and M_{22} mapping images (top) and histograms (bottom) of mature fig

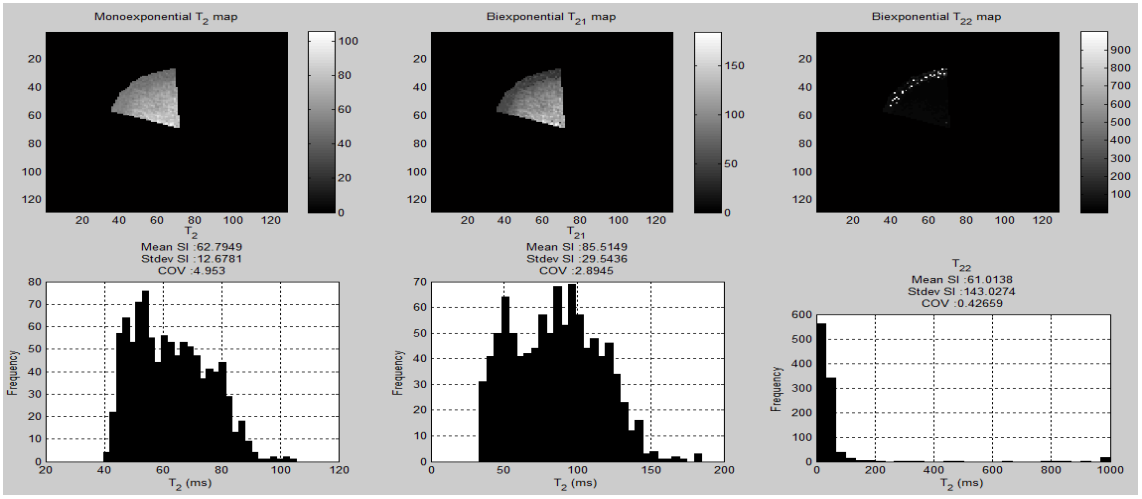

Figure 3: Processed T_2, T_{21}, and T_{22} mapping images (top) and histograms (bottom) of immature fig

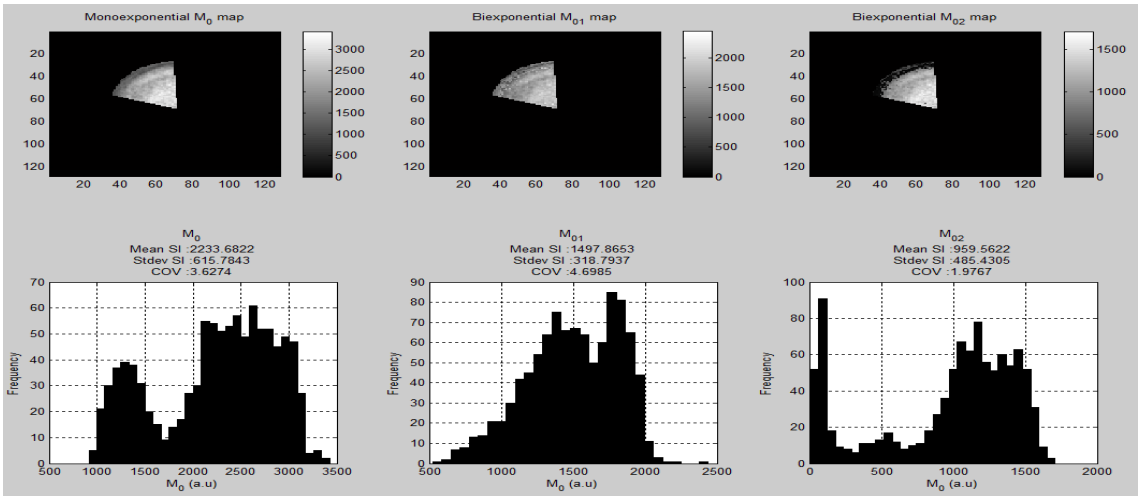

Figure 4: Processed M_0, M_{21}, and M_{22} mapping images (top) and histograms (bottom) of immature fig

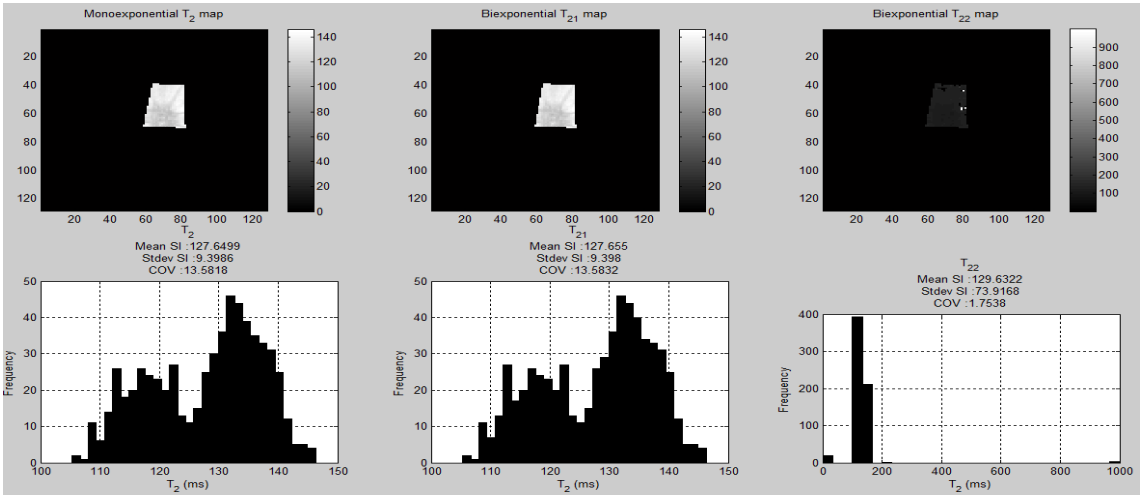

Figure 5: Processed T_2, T_{21}, and T_{22} mapping images (top) and histograms (bottom) of 'Fuyu' persimmon

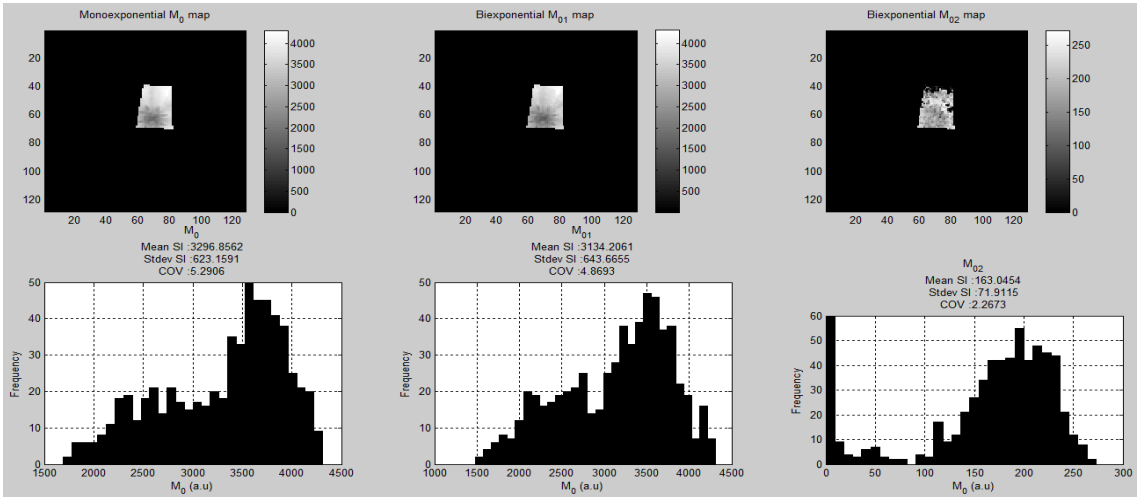

Figure 6: Processed M_0, M_{21}, and M_{22} mapping images (top) and histograms (bottom) of 'Fuyu' persimmon

To contrast a specific region of interest, e.g. decayed internal parts or abnormal tissues, in a sample we adjust magnetic resonance imaging parameters, TR and TE, when we use an MRI system. If we set long enough TR value, then TE is the key to contrast decayed parts. Finding optimal TE is not easy. In this case, if we can use MSME pulse sequence, it's very easy to find optimal TE value.

4. Conclusions

Using MSME imaging pulse sequence, magnetic resonance characteristics of various fresh fruits were examined easily. Magnetic parameters, T_2 and M_o, were closely related to physical state changes of fresh fruits. This method suggests a useful way to contras region of interest (ROI) in a simple way when using MRI. The results suggest convenient ways of designing magnetic resonance experiments or sensors based on magnetic resonance techniques. Further studies are needed for specific applications of magnetic resonance techniques.

Acknowledgements

This work was supported by the Center for IT Convergence Agricultural Machinery (ITAM) grant (No. R14-3) funded by the Ministry of Trade, Industry and Energy, Korea.

References

Andaur J.E., Guesalaga A.R., Agosin E.E., Guarini M.W., Irarrazaval P, 2004, Magnetic resonance imaging for non-destructive analysis of wine grapes, J. Agric. Food Chem., 52, 165-170.

Butz P., Hofmann C., Tauscher B., 2005, Recent developments in noninvasive techniques for fresh fruit and vegetable internal quality analysis, J. of Food Science, 70(9), 131-141.

Chen P., McCarthy M.J., Kauten R., 1989, NMR for internal quality evaluation of fruits and vegetables. Transactions of the ASAE, 32(5), 1747-1753.

Defraeye T., Lehmann V., Gross D., Holat C., Herremans E., Verboven P., Verlinden B., Nicolai BM., 2013, Application of MRI for tissue characterisation of 'Braeburn' apple, Postharvest Biology and Technology, 75, 96-105.

Gadian D.G., 1995, NMR and its applications to living systems. Oxford University Press Inc., New York, USA,

Kim S.M., Chen P., McCarthy M.J., Zion B., 1999, Fruit internal quay evaluation using on-line nuclear magnetic resonance sensors. J. of Agricultural Engineering Research, 74(3), 293-301.

Kim S.M., Milczarek R., McCarthy M.J., 2008, Fast detection of seeds and freeze damage of mandarins using magnetic resonance imaging, Modern Physics Letters B, 22(11), 941-946.

McCarthy M.J., 1994, Magnetic resonance imaging in foods. Chapman and Hall, London, U.K.

Milczarek R., 2009, Multivariate image analysis: An optimization tool for characterizing damage-related attributes in magnetic resonance images of processing tomatoes. PhD dissertation, University of California, Davis, CA., USA.

Zhang L., McCarthy M.J., 2013, Assessment of pomegranate postharvest quality using nuclear magnetic resonance, Postharvest Biology and Technology, 77, 59-66.